

Jet formation model from accretion disks of electron-ion-photon gas

E. Katsadze^a, N. Revazashvili^a, N. L. Shatashvili^{a,b}

^aDepartment of Physics, Faculty of Exact and Natural Sciences, Javakishvili Tbilisi State University (TSU), Tbilisi 0179, Georgia

^bTSU Andronikashvili Institute of Physics, TSU, Tbilisi 0177, Georgia

Abstract

The problem of Astrophysical Jet formation from relativistic accretion disks through the establishment of relativistic disk-powerful jet equilibrium structure is studied applying the Beltrami-Bernoulli equilibrium approach of Shatashvili & Yoshida 2011; Arshilava et al. 2019. Accretion disk is weakly magnetized consisting of fully ionized relativistic electron-ion plasma and photon gas strongly coupled to electrons due to Thompson Scattering. Analysis is based on the generalized Shakura-Sunyaev α -turbulent dissipation model for local viscosity (being the main source of accretion), in which the contributions from both the photon and ion gases are taken into account. Ignoring the self-gravitation in the disk we constructed the analytical self-similar solutions for the equilibrium relativistic disk-jet structure characteristic parameters in the field of gravitating central compact object for the force-free condition. It is shown, that the magnetic field energy in the Jet is several orders greater compared to that of accretion disk, while jet-outflow is locally Super-Alfvénic with local *Plasma-beta* < 1 near the jet-axis. The derived solutions can be used to analyze the astrophysical jets observed in binary systems during the star formation process linking the jet properties with the parameters of relativistic accretion disks of electron-ion-photon gas.

Keywords:

Accretion, accretion discs, Galaxies: jets, Galaxies: structure

1. Introduction

Observations suggest that the star formation process is often accompanied by the accretion disk (AD), with the significant intrinsic link found to the strong bipolar/unipolar outflows/jets/winds streaming out from them carrying away the matter, energy and angular momentum of the accreting matter, thus effectively promoting the development of a star and playing the important role in the disk-evolution (Blandford & Rees 1974; Ustyugova et al. 1999; Dullemond et al. 2007). When the accretion rate is sub-Eddington and the opacity very high, the standard thin accretion disk is formed. It is geometrically thin in the vertical direction and is made of a relatively cold gas, with a negligible radiation pressure. Properties of AD-jet outflow systems can be explored from the observations of: young stellar objects (YSOs, Herbig-Haro (HH) objects, T-Tauri and Herbig Ae/Be stars) as well as of the galactic objects (black holes (BH), neutron stars, white dwarfs (WD)), extragalactic supermassive BHs and their disks. Thin disk is not always formed, specifically in the case of BHs Binaries and X-ray Binaries (of which disk is mostly optically thin while the polar regions of compact object can be either optically thin or optically thick – e.g. case of X-Ray Pulsars, BH-s) (see e.g. (Hartmann 2009; Ferreira 2008; Mirabel & Rodriguez 1999) and references therein).

It is expected, that large-scale outflows met in various active astrophysical objects being the collimated long-lived structures related to accreting disks surrounding the central compact objects [see e.g. (Begelman et al 1984) and references therein] are playing an important role in stellar evolution, including late

stages of their lives and their final fates. The most luminous objects of the Universe (observed in different classes of narrow binary systems as well as Active Galactic Nuclei (AGNs) and quasars) are fed by accretion of matter onto central compact objects. It is believed that many stars are born in the binary systems going through one or more phases of the mass-exchange (Winget & Kepler 2008; Kawka & Vennes 2014; Tremblay et al 2015; Mukai 2017). Numerous observed accreting WDs are often surrounded by an accretion gas of companion star / disk (Begelman et al 1984; Mukai 2017). Cataclismic Variables (CVs) and Symbiotics are representing the accreting white dwarf binaries (AWBs) being important laboratories for accretion and outflow physics. In nova-like CVs the outflow velocities can vary within 200-5000 km/s (Long et al 2002; Kafka & Honeycutt 2004; Puebla et al 2011).

It is well-known that magnetic fields play important roles in accelerating jets in different ways (Blandford & Rees 1974; Uchida & Shibata 1985; Shibata & Uchida 1986; Kudoh & Shibata 1997); also the gas pressure may become important in some cases (Takahara et al. 1989; Takasao et al. 2017), being often dominant in the disks specifically for weakly magnetized cases (Koide et al. 1998; Widrow 2002). Then, the observable properties of jets/outflows as well as the ADs depend not only on the accretion mechanism in disk but on the jet-acceleration mechanism as well. Therefore, one has to consider both heating and acceleration mechanisms in the unified approach in addition to the formation stage of jets for better comparisons between theoretical models and observations (Zanni et al. 2007; Takasao et al. 2017). At the same time the

main mass/energy source of the ejecta is the disk-flow material/energy released through the accretion process. Hence, jet velocities are intrinsically correlated with the accretion rates dependent on the unified disk-jet system dynamics; the central object dynamics may play the additional role in the formation of relativistic outflows/jets [Livio 1997– powerful jets are produced by systems in which on top of an accretion disk threaded by a vertical field, there exists an additional source of energy/wind, possibly associated with the central object (for example, stellar wind from protostar may accelerate YSO jets, as estimated by Ferreira 1997; Ferreira et al. 2006, 2007)].

AGNs, hosting super-massive accreting black holes, are commonly (Barnier et al. 2023; Del Santo et al. 2023) believed to be powered by an optically thick, geometrically thin AD that emits in the optical and UV energy range (Shakura & Sunyaev 1973); some of which also show hard X-ray emission that is assumed to result from the disk photons Compton scattering off thermal electrons in the so-called hot corona, located somewhere near the BH. According to Barnier et al. 2023, when the local magnetization is high, the effect of the formed jets on the disk structure can be tremendous since the jets’ torque efficiently extracts the disk angular momentum, significantly increasing the accretion rate. As a result such Jet Emitting Disk (JED) has a much lower density in comparison to the standard accretion disk (SAD) and produces the hard X-ray emission attributed to the hot corona. The parameter space for stationary JED solutions correspond to magnetization in the range $[0.1, 1]$. In the outer region, where the magnetization is small ($\ll 1$) a SAD (Shakura & Sunyaev 1973) is present.

As mentioned above, the observable properties of jets, such as the local velocities, energies, opening angle, mass-loss rate depend on their formation mechanism, AD characteristic properties and dynamical acceleration as well as heating mechanisms. Moreover, we know that morphology, geometry and velocities of the jets can be used to estimate the mass, luminosity and/or age of the YSOs (see Bally 2016 and references therein) and compact objects (see e.g. Begelman 1998; Celloti & Blandford 2001. Explorations of the jet-outflows (see, e.g., Ioannidis & Froebrich 2012; Smith et al. 2014; Zhang et al. 2014 for YSOs) provide an unbiased observational data that can be used to test the theoretical models of the equilibrium disk-jet structures. In (Shatashvili & Yoshida 2011) it was shown, that there exists a general principle that dictates a marked similarity in macroscopic accreting disk-jet outflow geometry despite the huge variety of the scaling parameters such as Lorentz factor, Reynolds number, Lundquist number, ionization fractions, etc., characterizing different systems indicating that magnetic field (pre-existed or generated) could play crucial role in jet-acceleration and its collimation, and not for disk-jet structure formation (see in addition Yoshida & Shatashvili 2012; Arshilava et al. 2019). For the jet acceleration the magnetic mechanism (when the global poloidal magnetic fields are twisted by the rotating disk to the azimuthal direction, extracting angular momentum from the disk, enabling efficient accretion of disk plasmas onto BH and forming bipolar relativistic jets that are also collimated by the magnetic force) was proposed

not only for AGN jets (Lovelace 1976; Krasnopolsky et al. 1999; Pelletier et al. 1971; Meier et al. 1994) but also for protostellar jets (Pudritz & Norman 1986; Uchida & Shibata 1985; Shibata & Uchida 1986; Ouyed et al. 1997). The studies on the dynamical formation of relativistic outflows (jets) (e.g. O’Dell 1981; Begelman et al 1984; Sikora & Wilson 1981; Phiney 1982) from highly luminous radiation sources, such as AGNs or compact galactic objects show the connection of jet formation with GRBs in quasars/microquasars (Mirabel & Rodriguez 1999; Barnier et al. 2023; Del Santo et al. 2023) since electrons and photons are coupled due to Thompson Scattering (Peebles 1969, 1980, 1993; Widrow 2002). Recent studies (Yang et al. , 2024) indicate that observed AGN jets are driven by the Blandford & Znajek 1997 mechanism.

In (Arshilava et al. 2019) the theoretical model for the disk-jet structure formation for YSOs was developed based on the Beltrami Flow model of (Shatashvili & Yoshida 2011) using the turbulent viscosity (Shakura & Sunyaev 1973) as the main reason of accretion; disk was assumed un-magnetized (no pre-existed global magnetic field was considered). Analytical conditions for disk-jet structure formation and parameter ranges for jet-launching and collimation for YSO Jets were found. The derived solutions describe the astrophysical disk-jet structures with low ionization, where the main energy source of the outflow should come from non-magnetic processes. It was shown that formed disk-jet structure depends on the thermal properties of disk-flow and the outflow local Mach number depends on the background pressure in the jet area.

In the present paper we extend the theoretical study of (Arshilava et al. 2019) for jet-formation from SAD with electron-ion-photon gas using the generalized turbulent viscosity approach of (Shakura & Sunyaev 1973) in which the dissipation includes both the photon gas and ion gas contributions being the main source of accretion. Ignoring the self-gravitation in the disk we constructed the analytical self-similar solutions for the equilibrium relativistic disk-jet structure characteristic parameters (velocity field, generalized vorticity, magnetic field, Alfvén Mach number, plasma-beta) in the field of gravitating central compact object for the force-free condition justified by observations for our system of study. AD is weakly magnetized and consists of fully ionized relativistic electron-ion plasma and photon gas strongly coupled to electron gas due to Thompson Scattering, often met in different binary systems. Hence, photon gas behaves as a charged fluid and problem reduces to the study of relativistic three-fluid system; the effects of compact object magnetic field that may influence the disk formation process, and hence, the equilibrium disk-jet structure formation (Hartmann 2009; Barnier et al. 2023) are ignored.

2. Physical Model and Equations for Disk-Jet Structure

In our model accretion disk consists of fully ionised electron-ion plasma and photon gas strongly coupled to electron gas due to Thompson Scattering (see e.g. Peebles 1980; Widrow 2002; Hartmann 2009; Harrison 1973 and references therein) often

met in different binary systems. To describe corresponding astrophysical disk-jet object we use relativistic equations for three fluids [below subscripts i , e and γ are used for ions, electrons and photons, respectively; electron-ion collisions are ignored] (Weinberg 1972; Baierlein 1978; Peebles 1980):

$$\rho_i \frac{d\mathbf{v}_i}{dt} = -\nabla p_i + \frac{en}{c} (\mathbf{E} + \mathbf{v}_i \times \mathbf{B}) + \rho_i \nu_i \nabla^2 \mathbf{v}_i + \rho_i \nabla \Phi, \quad (1)$$

$$\rho_e \frac{d\mathbf{v}_e}{dt} = -\nabla p_e - \frac{en}{c} (\mathbf{E} + \mathbf{v}_e \times \mathbf{B}) + \frac{4}{3} \frac{\rho_\gamma}{t_{\gamma e}} (\mathbf{v}_\gamma - \mathbf{v}_e) - \rho_e \nabla \Phi, \quad (2)$$

$$\frac{4}{3} \rho_\gamma \frac{d\mathbf{v}_\gamma}{dt} = -\frac{c^2}{3} \nabla \rho_\gamma - \frac{4}{3} \frac{\rho_\gamma}{t_{\gamma e}} (\mathbf{v}_\gamma - \mathbf{v}_e) + \frac{4}{3} \rho_\gamma \nu_0 \nabla^2 \mathbf{v}_\gamma - \frac{4}{3} \rho_\gamma \nabla \Phi, \quad (3)$$

where ρ_i, ρ_e and ρ_γ are the densities of ion, electron and photon fluids and ν_i and $\nu_0 (= 2/9n\sigma_T)$ are the ion and photon fluid's turbulent viscosities, respectively (Chan & Jones, 1975): $t_{\gamma e} = 1/(nc\sigma_T)$ is the photon-electron collision time, $n = n_i = n_e$ is the ion (electron) proper number-density for fully ionized gas; $\sigma_T = 6.65 \cdot 10^{-25} \text{cm}^2$ is the Thomson cross-section; Φ is the gravitational potential of the central compact object; it is assumed, that the self-gravity of disk can be ignored.

For our problem of interest we ignore the electron inertia and summing up equations (2, 3), ignoring electron fluid stresses compared to those for photon fluid, we arrive to the so called "charged photon" fluid equation of motion (see Harrison 1973; Baierlein 1978 and references therein):

$$\frac{4}{3} \rho_\gamma \frac{d\mathbf{v}_\gamma}{dt} = -\nabla p_\gamma - \frac{en}{c} (\mathbf{E} + \mathbf{v}_e \times \mathbf{B}) + \frac{4}{3} \rho_\gamma \nu_0 \nabla^2 \mathbf{v}_\gamma - \frac{4}{3} \rho_\gamma \nabla \Phi, \quad (4)$$

where $p_\gamma = (c^2/3)\rho_\gamma$ is the photon fluid pressure.

Accreting AD (e.g. YSO disk) – jet structure, according to observations, is quite a long-lived object and the steady state solutions could well describe its behavior. Then, from the equations (1, 4), one can write the equation governing the dynamics of the stationary compressible magnetised multi-component fluid rotating around a central massive gravitating object as a whole in the following form:

$$\rho (\mathbf{v} \cdot \nabla) \mathbf{v} = -\nabla \mathcal{P} + \frac{1}{c} \mathbf{j} \times \mathbf{B} + \frac{4}{3} \rho_\gamma \left(\nu_0 + \nu_i \frac{4n m_i}{3\rho_\gamma} \right) \nabla^2 \mathbf{v} - \rho \nabla \Phi, \quad (5)$$

where

$$\mathcal{P} \simeq p_i + p_\gamma, \quad (6)$$

is the total thermodynamic pressure,

$$\mathbf{j} = en (\mathbf{v}_i - \mathbf{v}_e), \quad (7)$$

is the current density and we have introduced for the total density ρ and common velocity \mathbf{v} for the combined system of ion and electron-photon fluid the following

$$\rho = \frac{4}{3} \rho_\gamma + \rho_i, \quad (8)$$

and

$$\rho \mathbf{v} = \frac{4}{3} \rho_\gamma \mathbf{v}_\gamma + \rho_i \mathbf{v}_i. \quad (9)$$

We need to add here the Maxwell equations, Equations of State and Continuity Equations for each fluid. To find the Equation for magnetic field we recall that we consider the disk (or its regions) such that its magnetic field (large scale) is weak so that its energy is much smaller than the fluid energy and, hence, back-reaction of the magnetic field on the turbulent viscosity (that is the reason for the accretion) is small and we can ignore the Hall term in the equation (5) (i.e. we apply below the force-free condition).

Since the photon fluid, as mentioned above, is strongly coupled with electron fluid due to Thomson scattering, as if it is a "charged photon" fluid, we do not distinguish with photons and electrons and simply have:

$$\mathbf{v}_\gamma \approx \mathbf{v}_e = \frac{3}{4} \frac{1}{\rho_\gamma} (\rho \mathbf{v} - \rho_i \mathbf{v}_i), \quad \mathbf{j} = e \frac{\rho}{m_i} (\mathbf{v} - \mathbf{v}_\gamma). \quad (10)$$

Taking the curl of Eq. (2) and ignoring the heating/cooling of electron fluid (not important in equilibrium state, specifically when the generation of short-scale fields is ignored) due to Biermann effect, we arrive to:

$$\nabla \times \mathbf{v}_e \times \mathbf{B} = 0$$

leading to following Beltrami condition for charged photon fluid (electron/photon-fluid is frozen into the magnetic field):

$$\mathbf{v}_\gamma \parallel \mathbf{B}, \quad \mathbf{v}_\gamma = \mu_\gamma \mathbf{B} \quad (11)$$

where the Beltrami parameter μ_γ is a scalar function satisfying the condition:

$$(\mathbf{v}_\gamma \cdot \nabla) \frac{1}{\mu_\gamma} = 0 \quad (12)$$

and, hence, the condition for the force-free magnetic field can be written as:

$$\mathbf{j} \times \mathbf{B} = 0 \implies \nabla \times (\rho \mathbf{v}) \times \mathbf{B} = 0. \quad (13)$$

Note, that the equations (5) and (13), together with stationary Continuity equation $\nabla \cdot (\rho \mathbf{v}) = 0$ and Maxwell equation $\nabla \cdot \mathbf{B} = 0$, are the equations describing the one fluid MHD in the force-free regime, no two-fluid effects like the generation of short-scale fields (of both magnetic and velocity nature (Mahajan et al 2001; Berezhiani et al 2015)) are taken into account; such effects we will study in our future investigations, as they are important for the Unified Dynamo/Reverse Dynamo (Mahajan et al 2005, 2006; Kotorashvili et al 2020; Kotorashvili & Shatashvili 2022) and heating processes (Mahajan et al 2001), as well as

the catastrophic acceleration/amplification of velocity/ magnetic fields (Ohsaki et al 2001, 2002; Mahajan et al. 2002; Barnaveli & Shatashvili 2017) leading to the modification of dissipation effects (hence, of accretion) but not important for the formation of minimal (universal) disk-jet structure. Hence, knowledge of composite fluid momentum $\mathbf{P} = \rho\mathbf{v}$ for considered AD is fully sufficient for the definition of magnetic field (large-scale) in the minimal model. The assumption for force free magnetic field for the 3-fluid system of disk regions where the large-scale magnetic energy is smaller than the flow energy made this possible. The opposite limit constitutes a different problem, which can work for the areas of inner disk-edge close to the compact object with strong magnetic fields affecting the disk formation/disk's local magnetic field (see e.g. Ferreira (2008); Tout et al (2008) and references therein).

As shown in Arshilava et al. (2019); Shatashvili & Yoshida (2011); Yoshida & Shatashvili (2012) for disk-jet structure formation stage magnetic field is not necessary — having a distinguishable viscosity in the disk is enough to create the accretion, leading to the feeding of outflow/jet by disk-flow energy/material; magnetic field affects significantly the outflow/jet collimation and acceleration. In ideal MHD numerical simulations, it has been found that the magneto-rotational instability (MRI) generates turbulence (Balbus & Hawley, 1991), unless strong non-ideal effects in extremely low-ionized gases suppress MRI (Bai, 2016). Effect of the magnetic field on the local turbulence (that amplifies it) may become substantial only when magnetic energy grows so that it becomes comparable to the kinetic energy of the small-scale turbulence (important for disk-jet structure formation era) (Baierlein, 1978); then we may expect that in the minimal model of force-free field the formed disk-jet structure will remain similar to unmagnetized case. One can expect, that the two-fluid effects (Mahajan et al 2001, 2006) in disk (arising from $\mathbf{j} \times \mathbf{B} \neq 0$ – when matter is not current-less) will effectively modify the local accretion due to the creation of large short-scale magnetic fields feeding turbulence/anomalous viscosity (Baierlein 1978; Mahajan et al 2001); also in equilibrium the Biermann battery effect can be neglected (Widrow, 2002) for electron-fluid (as performed above), as well as the effects of heating/cooling. These effects as well as the non-force-free regimes for corresponding disk-regions we will consider in our future studies.

Then, problem of finding the magnetic field for our scenario is reduced to the problem of finding the fluid-flux/momentum $\mathbf{B} \sim \rho\mathbf{v}$ – the large-scale magnetic field behaves similar to the total current (flux for the flow, that is a momentum \mathbf{P}). We need to find the behaviour of velocity field and formulate the constraint on Beltrami parameter for entire composite flow: $\rho\mathbf{v} = \mu\mathbf{B}$ with $\mu \gg 1$; the results of opposite range ($\mu \ll 1$ for the strongly magnetized disk case) will be studied elsewhere; working out the consequences of related phenomenon for disk-jet structure formation is underway.

It is interesting to note, that the governing equations for our geometrically thin disk with rotating composite system of ion fluid and "charged photon fluid" in stationary state are reduced to the equations that describe the neutral rotating disk matter around the compact object studied in Arshilava et al.

(2019), with ρ , \mathbf{P} , ν , \mathcal{P} representing the characteristic parameters of composite fluid and the accretion caused mainly due to the photon fluid viscosity (although the generalized viscosity includes both the photon gas contributions as well as of ions the role of ions relative to photons is negligible in the local turbulent-viscosity (see e.g. Harrison 1973; Chan & Jones 1975; Baierlein 1978). Then, we can follow the above mentioned paper to find the velocity field of a disk fluid (as a whole) solving following equations:

$$(\mathbf{v} \cdot \nabla)\mathbf{v} = -\nabla h - \nabla\Phi + \frac{1}{\rho}\nabla \cdot \mathbf{T}, \quad (14)$$

$$\nabla \cdot (\rho\mathbf{v}) = 0, \quad (15)$$

where \mathbf{v} , ρ and h are the velocity, density and enthalpy of composite system, respectively; we have used the barotropic equation of state (for our problem of study) to calculate the enthalpy of the fluid:

$$\nabla h = \frac{1}{\rho}\nabla\mathcal{P}, \quad (16)$$

where the viscous stress tensor T_{ik} (now representing the total dissipative effects defining the accretion) and the corresponding term in Eq.(14) is formally written as:

$$\nabla \cdot \mathbf{T} \equiv \nabla_k T_{ik} = \frac{\partial}{\partial x_k} T_{ik}. \quad (17)$$

Following Shatashvili & Yoshida (2011); Yoshida & Shatashvili (2012), introducing a so-called "ideal" and "reduced" factors of "local" density (see also Arshilava et al 2019)

$$\rho = \rho_I \rho_R \quad (18)$$

to separate the ideal fluid and the dissipative effects and to track the accretion effects in disk-jet structure formation process so that $\rho_R = 1$ and $\rho_I = \rho$ in conventional ideal fluid mechanics with zero dissipation, we seek the steady state solutions of the disk-jet structures persisting around a central accreting slowly rotating compact object: The details of derivation of major analytical relations are presented in Appendix A.

Then, the stationary state of the rotating thin composite system of AD can be fully investigated using Eqs. (13,A.4,A.5, A.6) and the explicit form of the viscous stress tensor related to the specific object conditions. In present paper we employ the model in which the small scale turbulence creates the anomalous dissipation that can be described by using the generalized α -viscosity model introduced by Shakura & Sunyaev (1973) in which we use the effective viscosity model both in the disk and jet as well as in the disk-jet transition areas (Arshilava et al. 2019). Assuming the strong azimuthal rotation, splitting the pressure \mathcal{P} into the background constant component \mathcal{P}_0 and deviation form it p ,

$$\mathcal{P} = \mathcal{P}_0 + p, \quad (19)$$

the turbulent stress tensor can be split into the background constant component \bar{T}_{ik} and smaller varying deviation t_{ik} :

$$T_{ik} = \bar{T}_{ik} + t_{ik} \quad (20)$$

with $\bar{T}_{r\varphi} = \alpha_0 \mathcal{P}_0$, assuming axisymmetric flow $v_\varphi = r\Omega_K(r, z)$ rotating locally with Keplerian angular velocity (justified for the rotationally supported flow, for which the radial pressure gradients can be negligible compared to the centrifugal force – situation found for slowly accreting flows with slowly varying background pressure $\mathcal{P}_0 \simeq \text{const}$):

$$\Omega_K^2(r, z) = \frac{GM_\star}{(r^2 + z^2)^{3/2}}, \quad (21)$$

where M_\star is the mass of the central object, in the axisymmetric case, the only significant viscous stress tensor elements can be calculated as follows:

$$t_{r\varphi} = \frac{r^2}{r^2 + z^2} \beta p, \quad (22)$$

$$t_{z\varphi} = \frac{rz}{r^2 + z^2} \beta p, \quad (23)$$

where positive/negative p corresponds to the stronger/weaker turbulence compared to the background generalized turbulent steady state.

The geometry of the observed disk-jet structures and the continuity Eq. (15) dictate the expansion of the flow velocity in the following way (Shatashvili & Yoshida 2011; Arshilava et al. 2019):

$$\mathbf{v} = \frac{1}{\rho} (\nabla\psi \times \nabla\varphi) + rv_\varphi \nabla\varphi, \quad (24)$$

where the axisymmetric stream function ψ exactly matches the stream function of the actual momentum $\mathbf{P} = \rho\mathbf{v}$ of the bulk flow. Then, the straightforward algebra presented in Appendix A leads to the Generalized Bernoulli Condition and Beltrami Condition represented by the Eqs. (A.13, A.14, A.15) and (A.16) which constitute the final set of equations.

3. The similarity solutions for disk-jet structures

To construct the solutions representing disk-jet structure, following Shatashvili & Yoshida (2011), we introduce the orthogonal variables $\tau = z/r$ and $\sigma = \sqrt{r^2 + z^2}$ so that $\nabla\tau \cdot \nabla\sigma = 0$ leading to the obvious results for the Gravitational Potential to be $\Phi = \Phi(\sigma) = -\Omega_0^2/\sigma$ and the stream function to be dependent only on the τ variable ($\psi = \psi(\tau)$): thus, making it possible to separate the variables in the solution.

Then, after some straightforward algebra (see Appendix A), when seeking solution of the system assuming that describing physical variables ($p, \rho_I, \rho_R, \lambda$) can be factorized using the similarity variables (σ, τ) applying variable splitting ansatz (like e.g. $p(\sigma, \tau) = p_1(\sigma)p_2(\tau)$, see (Shatashvili & Yoshida 2011; Arshilava et al. 2019)), for the azimuthal velocity we obtain:

$$v_\varphi(\sigma, \tau) = V_{\text{Kep}} = \frac{\sigma_0 \Omega_0}{(1 + \tau^2)^{1/2}} \left(\frac{\sigma}{\sigma_0} \right)^{-1/2}, \quad (25)$$

where Ω_0 is the Keplerian angular velocity of the rotation at some characteristic radius σ_0 in the disk. Then, applying this ansatz we find the explicit solutions for all ($p, \rho_I, \rho_R, \lambda$) in the σ coordinate. After finding the radial profiles of these parameters

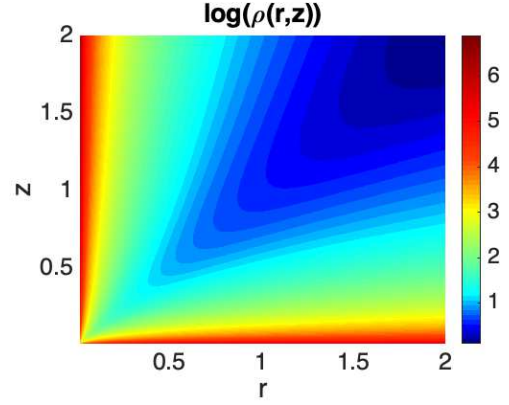


Figure 1: Total density $\rho(r, z)$ distribution of the weakly magnetized disk-jet structure for: $A_d = 3, A_j = 3, m_d = -3, m_j = 3$ and $\tau_0 = 0.01$; for $\rho_2(\tau)$ the power-law distribution (A.33) was used (compare with density distribution [Figure 4] of the unmagnetized disk-jet structure of (Arshilava et al. , 2019).

one derives the defining algebraic equation (A.26) which links the values of β parameter (defining the generalized viscosity of our composite 3-fluid system), τ -dependent part of density ρ_2 and the stream-function ψ , and represents the "realizability" condition for all existing solutions within the considered Beltrami flow model of disk-jet structure formation (the details can be found in Appendix A).

Then, applying the same methodology as studied in (Arshilava et al. , 2019) the general solutions of our weakly magnetized disk-jet model can be easily calculated - (see the Eqs. (A.29-A.32)) which together with the radial profiles and appropriate choice of the solution for W give the full solution for the disk-jet bulk (ion and electron-photon) flow for different types of density profiles $\rho_2(\tau)$ for which we employ the power-law distribution (cf. Shatashvili & Yoshida 2011). Figure 1 shows the total density (dimensionless) distribution of the weakly magnetized disk-jet structure. One can imagine that constructing the solution for only ion density one would find it different (in numbers) from the total density, although, geometrically similar to the total density presented above since the considered model dictates such solution.

Finally we obtain the velocity field components of the weakly magnetized disk flow (of composite 3 -fluid system consisting of ion, electron and photon gases):

$$v_{rD}(\sigma, \tau) = -\frac{2}{5} \frac{\tau^2}{(1 + \tau^2)^{3/2}} \left(\frac{\sigma}{\sigma_0} \right)^{-1/2} \beta \sigma_0 \Omega_0, \quad (26)$$

$$v_{zD}(\sigma, \tau) = -\frac{2}{5} \frac{\tau^3}{(1 + \tau^2)^{3/2}} \left(\frac{\sigma}{\sigma_0} \right)^{-1/2} \beta \sigma_0 \Omega_0, \quad (27)$$

and the jet flow:

$$v_{rJ}(\sigma, \tau) = \frac{5}{2} \frac{1}{(1 + \tau^2)^{1/2}} \left(\frac{\sigma}{\sigma_0} \right)^{-1/2} \frac{\sigma_0 \Omega_0}{\beta}, \quad (28)$$

$$v_{zJ}(\sigma, \tau) = \frac{5}{2} \frac{\tau}{(1 + \tau^2)^{1/2}} \left(\frac{\sigma}{\sigma_0} \right)^{-1/2} \frac{\sigma_0 \Omega_0}{\beta}. \quad (29)$$

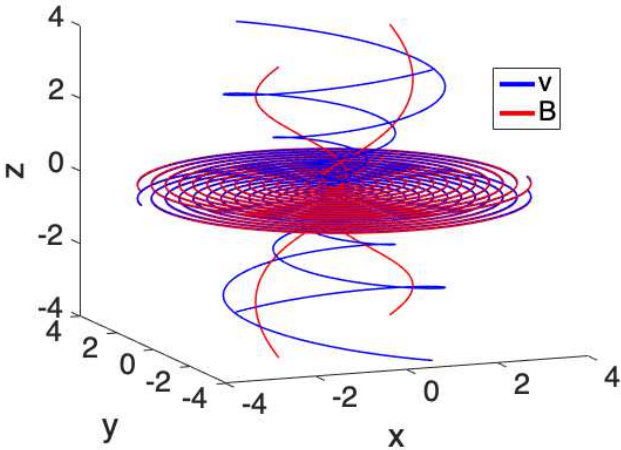


Figure 2: Velocity streamlines (blue) of the disk-jet structure illustrating accretion-ejection flow and global disk-jet magnetic field (red) at $\tau_d = 1$, $\tau_j = 2$, $\tau_0 = 0.01$, $\beta = 0.01$, $\kappa = 0.001$. Swirling of the velocity field is stronger than that of the magnetic field for the weakly-magnetized disk assumption.

Estimating the accretion speed of the flow in the disk region ($\tau < \tau_d$):

$$v_{\text{acc}} = (v_{rD}^2 + v_{zD}^2)^{1/2} = \frac{2}{5} \beta V_{\text{Kep}} \frac{\tau^2}{(1 + \tau^2)^{1/2}}, \quad (30)$$

and ejection velocity in the jet region ($\tau > \tau_j$):

$$v_{\text{ej}} = (v_{rJ}^2 + v_{zJ}^2)^{1/2} = \frac{5}{2} \frac{V_{\text{Kep}}}{\beta} (1 + \tau^2)^{1/2}. \quad (31)$$

we conclude, that in the low β limit derived solution corresponds to the locally slowly accreting flow ($v_{\text{acc}} \ll V_{\text{Kep}}$) in the disk with the locally fast outflow in the jet ($v_{\text{ej}} \gg V_{\text{Kep}}$), matching the properties of astrophysical accretion-ejection flows. Notice, that above expressions do not depend on the explicit profile of τ -dependent part of density (see Arshilava et al. 2019). Then, the continuous velocity field of bulk flow (as well as the continuous magnetic field via the relation (13)) can be calculated using Eqs. (A.31), (A.32) with the three region solution for the $W(\tau)$ function. For the magnetic field solutions we can employ stationary Continuity Equation ($\nabla \cdot \rho \mathbf{v} = 0$ and $\nabla \cdot \mathbf{B} = 0$, which, together with $\rho \mathbf{v} = \mu \mathbf{B}$ with $\mu \gg 1$ for our weakly magnetized disk yield

$$(\mathbf{v} \cdot \nabla) \frac{1}{\mu} = 0 \quad \implies \quad \frac{\partial}{\partial \tau} \mu = \text{const}$$

leading to $\mu^{-1} \simeq \kappa \tau$ with $\kappa \ll 1$ for our model (with variables splitting ansatz for similarity solutions). Figure 2 illustrates the streamlines of composite flow (blue) and global magnetic field (red) of the derived weakly magnetized disk-jet structure. Notice, that the construction of Velocity field doesn't require knowledge of density profile while magnetic field in our weak-field approximation with force-free condition needs

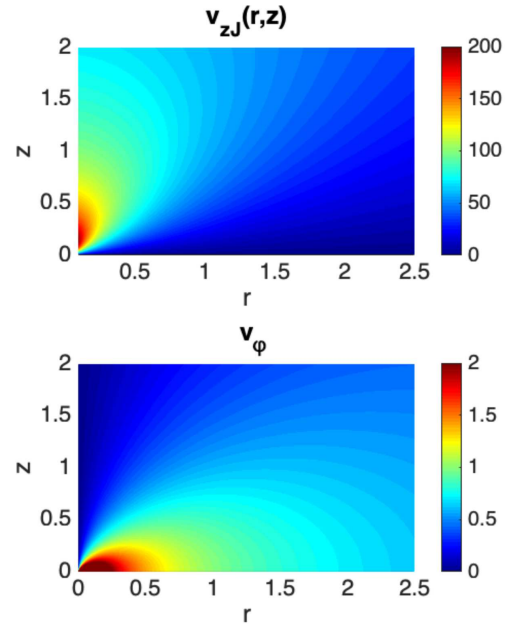


Figure 3: Profiles of the vertical velocity of the relativistic jet solution $v_{zJ}(r, z)/(2.5\sigma_0\Omega_0)$ (see Eq. (29)) (top) and the azimuthal velocity $v_\phi = V_{\text{Kep}}/(\sigma_0\Omega_0)$ in the disk (bottom) for $\beta = 0.01$. Maximal velocity of the outflow is reached near the vertical axis above the disk plane, at the top edge of TR while the maximal value of azimuthal (Keplerian) velocity is reached near the inner edge of a disk at the bottom edge of the TR at the disk mid-plane.

the density-profile to be known; also, swirling of the composite flow is faster than that of the magnetic field – this could be expected since only electrons are coupled with photons and not the entire e-i plasma, difference in the corresponding characteristic length-scales for ions and electrons shall cause this departure. It is interesting that numerous numerical runs showed no dependence of swirling ratio on κ for these vector-fields.

Disk-Jet structure configuration we constructed in present paper is a large-scale equilibrium structure the formation of which, as shown in (Arshilava et al. , 2019), is guaranteed for accretion-ejection flows with turbulent viscosity; the inclusion of weakly magnetized disk and photon gas effects extends the model for wider class of disk-jet structure systems. Observations also show, that geometrically all disk-jet structures show the universal geometrical character; the collimation efficiency of the jet is significantly defined by the acceleration mechanisms and magnetic field – we emphasize here, that the formation of jet and its further acceleration are different stages in the dynamics of the jet-evolution and, as shown in (Shatashvili & Yoshida , 2011; Arshilava et al. , 2019), for the minimal model there is no need in magnetic field for the jet-formation era.

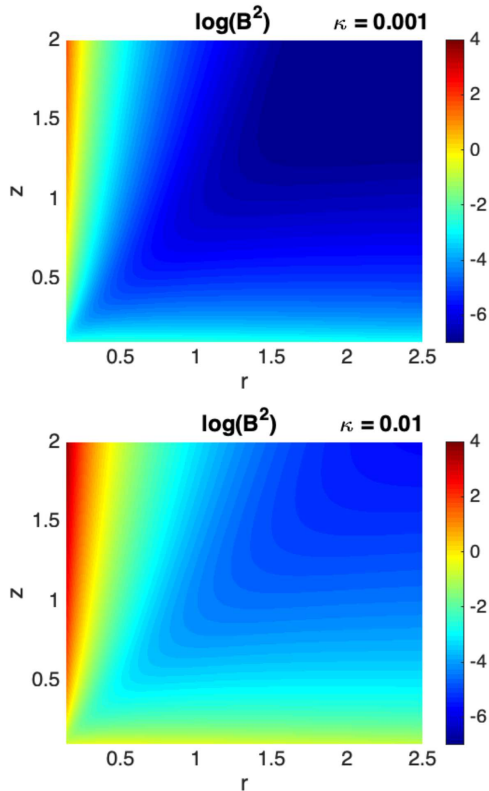


Figure 4: Magnetic Energy [$\log(B^2)$] normalized to p_0 for $\beta = 0.01$ plotted for different κ -s. The accumulation of magnetic energy in the Jet region is clearly seen reaching maximal values at the jet (vertical) axis; process is stronger for larger κ ; the jet region magnetic field is several orders greater compared to its disk area values. For density the distribution of Figure 1 was used.

4. Characteristic physical parameters of the constructed weakly magnetized disk–relativistic jet structure

In this section we present the illustrations for the characteristic parameters of the weakly magnetized disk–relativistic jet structure based on the solutions derived in the present paper emphasizing that the specific value of the local generalized viscosity β parameter can be found from observations for the concrete disk–jet object for which both the radial accretion and the vertical ejection velocities nearby the central object could be measured. From the Eqs. (30) and (31) we find $\beta^2 \sim v_{\text{acc}}/v_{\text{ej}}$ and since the value of $\beta (< \alpha_0)$ parameter is constrained by α_0 (the parameter describing anomalous viscosity due to background stationary turbulence) one easily finds:

$$v_{\text{ej}} > 10^4 v_{\text{acc}}$$

using a typical value from observational luminosity $\alpha_0 \sim 0.01$ (see Arshilava et al. (2019) and references therein).

To illustrate the properties of our solutions for the weakly magnetized disk–relativistic narrow jet structure the vertical velocity distribution of the jet flow and the azimuthal velocity are plotted in Figure 3 (see Eqs. (29) and (A.23)) for $\beta = 0.01$ – compare with Figure 5 of (Arshilava et al. , 2019) (for which

$\beta = 0.002$ was used and not the indicated in its Figure caption parameter). The outflow/jet launching is at the bottom edge of transition region (TR), just above the disk–surface and reaches its maximal value at the top edge of TR beyond of which the vertical flow velocity v_z decreases both with vertical and radial distances, similar to the Keplerian profile ($\propto (\sigma/\sigma_0)^{-1/2}$). Hence, the solutions derived within the minimal Beltrami–Bernoulli flow model well describes the *formation* of the weakly magnetized disk–relativistic jet structure (similar to un–magnetized case of (Shatashvili & Yoshida 2011; Arshilava et al. 2019)). We remind the reader that in our model the effects of central object magnetic field/jets, disk–winds as well as the heating/cooling processes were not considered. We believe that invoking these effects as well as the two–fluid effects (as discussed above) the generalized Magneto–Beltrami–Bernoulli mechanism (Mahajan et al. 2002; Mahajan et al 2006) may further accelerate and collimate the jet–flow. Also, depending on the plasma condition near the central object the disk–jet connection point may differ (one needs to add the equation of state taking into account the collisional effects together with pair creation, eruptive/explosive effects and etc. (see e.g. Widrow 2002; Mirabel & Rodriguez 1999; Barnier et al. 2023; Blandford & Rees 1974; Celloti & Blandford 2001; Zanni et al. 2007; Mignone et al 2005; Mouchet et al 2012 and references therein); investigations of these issues are underway.

Constructing the local Mach Number the possibility of forming the supersonic outflow in the narrow jet region at $\tau \gg 1$ near the jet axis was discussed in Arshilava et al. 2019 where the feasibility of derived solution with the Laval nozzle mechanism was also shown; similar result will persist also for our composite electron–ion–photon gas outflow. Moreover, since the pressure variation is negative in the jet region ($p < 0$ for $W_-(\tau) < 0$) the swirling solution in the jet region leads to the decrease of sound speed increasing the local Mach number of the outflow; when adding the cooling effect (not considered in minimal Beltrami–Bernoulli flow model) such increase will be stronger widening the area of supersonic flow existence.

For our weakly magnetized AD model of composite 3–fluid system it is essential to follow the distribution of the Alfvén Mach number ($= v_z \sqrt{\rho}/B = v_z/(\kappa \tau \sqrt{\rho} v)$) and Magnetic Energy throughout the formed disk–jet structure. For this purpose we constructed the illustrating plots for these 2 physical parameters using our self–similar solutions; for the background pressure we used the normalization of the background pressure \mathcal{P}_0 on the pressure p of the self–similar solution (Arshilava et al. 2019) at $\sigma = \sigma_0$ and $\tau = \tau_j$ (see Eqs. (A.30, A.33)):

$$p_0 \approx \frac{5}{2} \frac{\sigma_0^{1/2} \Omega_0^2}{\beta^2} A_j \tau_j^{m_j}, \quad (32)$$

assuming that $\tau_0 \ll \tau_j$.

Figure 4 shows the distribution of magnetic energy throughout the equilibrium Disk–Jet structure. One observes the accumulation of magnetic energy in the narrow region of formed Jet (near its axis), this process is stronger for bigger κ reflecting the effect of initial conditions in the electron–ion–photon gas accre-

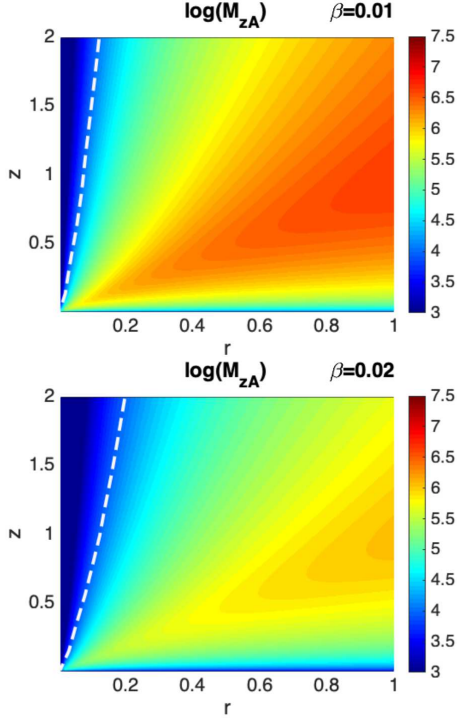


Figure 5: Vertical Alfvén Mach number of the jet flow $[\log(M_{zA}(r, z))]$ when $\tau_0 = 0.01$, $\kappa = 0.01$, $\sigma_0 = 1$ for different β -s ($= 0.01, 0.02$ from top to bottom). For density the distribution presented in Figure 1 was used. The flow is super-Alfvénic ($M_{zA} \gg 1$) everywhere decreasing with $\tau \gg 1$; with larger β the area of jet with $M_{zA}(r, z) < 10^4$ (see dashed line) gets wider; $M_{zA}(r, z)$ decreases along vertical axis indicating that radiation exists beyond the outflow major concentration span (compare with Figure 3).

tion disk; also note, that the jet region magnetic field is several orders greater compared to its disk area values. The plots for vertical Alfvén Mach number are illustrated in Figure 5 for different turbulent generalized viscosity parameter β for the specific $\kappa = 0.01$. One observes that the flow is super-Alfvénic ($M_{zA} \gg 1$) everywhere while its strength compared to magnetic energy reduces at $\tau \gg 1$; with larger β the area of jet with $M_{zA}(r, z) < 10^4$ (see dashed line) gets wider; $M_{zA}(r, z)$ decreases along vertical axis indicating that radiation exists beyond the outflow major concentration span. In Figure 6 the maximal values for magnetic energy in the jet (red) reached at the vertical axis and disk (blue) reached at the mid-plane of the disk are illustrated: (i) versus κ for different turbulent viscosity parameter β (*left panel*) and (ii) versus β for different κ -s (*right panel*). One clearly observes that the maximal values of magnetic energy are several orders larger in the jet compared to its values in the disk for all chosen cases. Moreover, the result is not sensitive to changes in β for the same κ while for the same β it increases gradually with κ – clear link to the initial preparation of the electron-ion-photon gas accretion disk / concrete conditions of specific astrophysical object.

Since in our model the effect of the central object magnetic field was not considered, it is expected that the final results for observed Alfvén Mach number (as well as the Magnetic Energy) in the jet region may decrease (increase) in the realistic

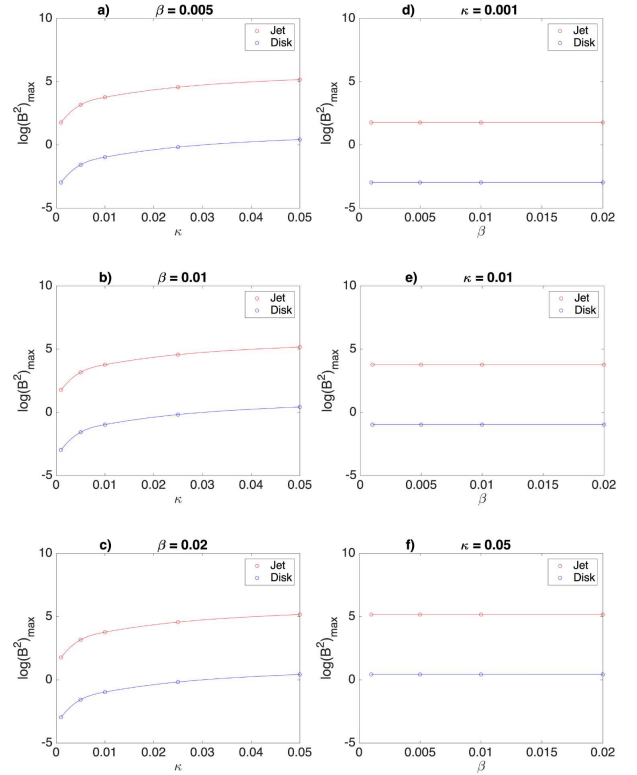


Figure 6: Maximal values of magnetic energy in jet (red) and disk (blue) for different turbulent generalized viscosity coefficients ($\beta = 0.005, 0.01, 0.02$) versus κ (see plots a), b), c) of the left column) and for different κ -s versus β (see plots d), e), f) of the right column); magnetic energy is several orders larger in jet compared to its value in the disk for all cases. Picture is not sensitive to changes in β for the same κ while for the same β it increases gradually with κ .

electron-ion-photon disk-relativistic jet systems; also the decrease of the generalized β parameter leads to the increase of the ratio between the vertical and radial velocities and, consequently, change of the equilibrium disk-jet flow/magnetic field geometry for various astrophysical objects. Even then, interestingly, the solutions derived in the minimal model considered in the present work applying Generalized Beltrami-Bernoulli flow model for equilibrium disk-jet structure, can well mimic slow radial sub-Keplerian accretion composite flow in the weakly magnetized disk region and fast narrow super-Keplerian collimated outflow with strong magnetic field in the jet region. As already discussed, inclusion of the above effects together with the Hall effect for stronger magnetic field regions will make the constructed disk-jet structure characteristic parameters closer to the realistic/observed astrophysical objects; prediction of the jet parameters will be more reliable as well.

To better illustrate the reliability of our approach we give the results for local plasma-beta parameter β_p in Figure 7 for the pressure ratio $\mathcal{P}_0/p_0 = 10^5$ for different local mag-

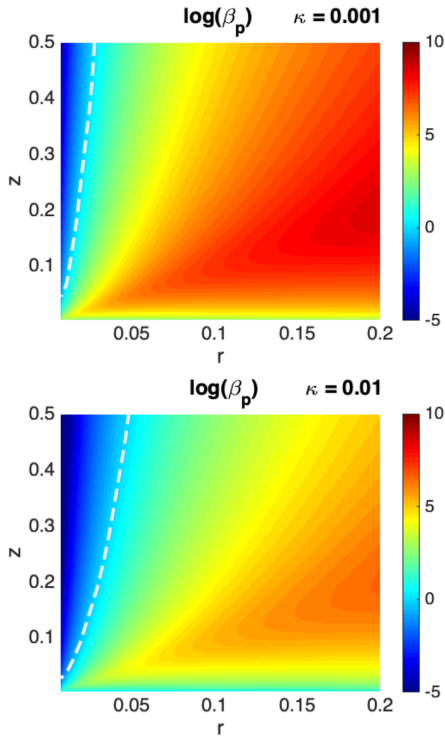


Figure 7: Plasma-beta β_p for turbulent generalized viscosity parameter $\beta = 0.01$ for $\kappa = 0.001$ (top), and $\kappa = 0.01$ (bottom) when $\tau_0 = 0.01$, $\beta = 0.01$; $\sigma_0 = 1$ and $\mathcal{P}_0/p_0 = 10^5$; the dashed line represents the place of $\beta_p = 1$ beyond which towards jet-axis ($\tau \gg 1$) the outflow $\beta_p < 1$. For density the distribution presented in Figure 1 was used.

netic field strengths (different κ -s) justified by observations. The dashed line represents the place of plasma $\beta_p = 1$ beyond which, towards jet-axis ($\tau \gg 1$), the outflow plasma-beta $\beta_p < 1$ (being at the same time supersonic close to axis); at wider angles ($\tau > 1$) the outflow plasma $\beta_p > 1$ (being subsonic) and, thus, should be decreasing away from the central object (from Figure 3 we observe $v_z(\sigma) \propto \sigma^{-1/2}$) (compare e.g. with Arce et al. (2013); Lee et al. (2018)). Notice, that bigger the local magnetic field strength (κ) larger is the area with plasma $\beta_p < 1$ in the jet (see e.g. Begelman et al. 1984; Vlemmings et al. 2007; Spruit 2010, 2011; Matsumoto & Tajima 1995; Matsumoto et al. 2004; Barnier et al. 2023; Koide et al. 1998 and references therein) for fixed viscosity parameter β . In fact, this effect shall become significant with inclusion of cooling (effect not considered in present approach) that will further reduce the local sound speed leading to the decrease in the local plasma-beta (with simultaneous increase of local Mach number (Arshilava et al. 2019)). This effect could add to the jet acceleration due to the farther adiabatic expansion; while in opposite limit the increase of the background pressure \mathcal{P}_0 would increase local plasma-beta (decrease the local Mach number to the subsonic values) changing the final geometry of disk-jet structure.

5. Summary

We extend the theoretical Beltrami-Bernoulli flow model of (Arshilava et al. 2019) for the relativistic jet-formation from SAD with electron-ion-photon gas using the Generalized Turbulent Viscosity approach (Shakura & Sunyaev 1973) in which the dissipation includes both the photon gas and ion gas contributions being the main source of accretion in the weakly magnetized disk while the star-formation process. Ignoring the self-gravitation in the disk we derived analytically the magnetized collimated jet outflow self-similar solutions for the force-free condition: for the stationary turbulent state (powering the accretion process both in the disk and jet of the unified equilibrium disk-jet structure in the field of gravitating central compact object) we constructed the characteristic parameters like velocity field, generalized vorticity, magnetic field, Alfvén Mach number, plasma-beta.

In our model the accretion disk is weakly magnetized and consists of fully ionized relativistic electron-ion plasma and photon gas strongly coupled to electron gas due to Thompson Scattering, often met in different binary systems. Hence, photon gas behaves as a charged fluid and problem reduces to the study of relativistic three-fluid system; the effects of compact object magnetic field that may influence the disk formation process, and hence, the equilibrium disk-jet structure final geometry, Hall term, as well as the heating/cooling and ionization modifying the local accretion were ignored. Also, in present analysis magnetized disk-winds were not invoked; the additional dissipation mechanisms as well as the phenomena in the vicinity of central object may play significant role too for the final physical parameters of formed disk-jet structure. We believe, that dynamical effects together with all above physical phenomena will make the solution of the problem only richer; the consequent problems of jet further acceleration as well as heating could be considered too (see e.g. (Ohsaki et al. 2001, 2002; Mahajan et al. 2002; Mahajan et al. 2006) for the possible jet-flow acceleration due to Hall effect in the generalized magneto-Bernoulli mechanism); study of these issues are planned for our future investigations.

Similar to un-magnetized case (Arshilava et al. (2019)) our relativistic magnetized disk-jet structure parameters depend on the thermal properties of the disk flow – the local Mach number of the jet-outflow depends on the background pressure in the jet area and at low pressure, jet outflow reaches supersonic amplitudes close to the central axis of the flow being transonic from low poloidal angles to higher poloidal angles decelerating with radial distance. Interestingly, the local Plasma-beta β_p shows opposite distribution – being > 1 in the disk it passes the value 1 at low poloidal angles and closer to jet axis it becomes < 1 ; such area is wider for bigger local background disk-magnetization (κ) (see e.g. Vlemmings et al. 2007; Spruit 2011; Matsumoto et al. 2004; Zanni et al. 2007; Koide et al. 1998) for fixed local viscosity. We observed the accumulation of magnetic energy in the narrow region of formed Jet (near its axis), being several orders greater compared to its disk area values; the result is not sensitive to changes in local generalized turbulent viscosity parameter β for the same background

magnetic fields while for the same β it depends on the background field in disk – this process is stronger for higher background magnetization of the disk reflecting the dependence on the initial conditions in the electron-ion-photon gas accretion disk. The results for vertical Alfvén Mach number show that the flow is super-Alfvénic ($M_{zA} \gg 1$) everywhere in the equilibrium relativistic disk-jet structure while the outflow kinetic energy decreases faster with vertical distance compared to magnetic energy as well as towards the axis; this picture depends on the background local disk-parameters (with larger β the area of jet with $M_{zA}(r, z) < 10^4$ gets wider).

Considered weakly magnetized accretion disk-relativistic jet solutions describe the formation of the high velocity magnetized jet from slowly accreting locally Keplerian electron-ion-photon disk-flow and can be used to analyze topological characteristics of Jets from binary systems linking them to the local physical conditions at the jet launching areas; since in the present study the clear link of outflow parameters to the background accretion disk conditions is well shown the predictions for observed structures are possible. The further kinematic acceleration and collimation of the jet flow may happen due to the effects not considered in the current minimal model.

Acknowledgments

Authors express special thanks to V.I. Berezhiani and A.G. Tevzadze for their valuable discussions. Present research was partially supported by Shota Rustaveli Georgian National Foundation Grant Project No. FR-22-8273.

Appendix A. Derivation of major analytical relations

Following Shatashvili & Yoshida (2011); Yoshida & Shatashvili (2012) we introduce a so-called “ideal” and “reduced” factors of “local” density (see also Arshilava et al 2019) to seek for the steady state solutions of the disk-jet structures persisting around a central accreting slowly rotating compact object:

$$\rho = \rho_I \rho_R \quad (\text{A.1})$$

to separate the ideal fluid and the dissipative effects and to track the accretion effects in disk-jet structure formation process so that $\rho_R = 1$ and $\rho_I = \rho$ in conventional ideal fluid mechanics with zero dissipation. The “ideal” and “reduced” momenta then read as:

$$\mathbf{P}_I = \rho_I \mathbf{v}, \quad \mathbf{P}_R = \rho_R \mathbf{v} \quad (\text{A.2})$$

and from the equations (14,15) we obtain a “Generalized Pressure Balance equation” in terms of the new momenta:

$$\begin{aligned} \mathbf{P}_R \times (\nabla \times \mathbf{P}_R) &= \quad (\text{A.3}) \\ &= \frac{1}{2} \nabla P_R^2 + \rho_R^2 \nabla (h + \Phi) + \frac{\rho_R}{\rho_I} [\mathbf{P}_R (\nabla \cdot \mathbf{P}_I) + \nabla \cdot \mathbf{T}]. \end{aligned}$$

Due to the geometry of the problem the natural assumption for the reduced momentum to obey the Beltrami Condition implying that the Reduced Momentum is aligning the corresponding

Generalized Vorticity is valid (see e.g. Arshilava et al. (2019) and references therein):

$$\mathbf{P}_R = \lambda (\nabla \times \mathbf{P}_R), \quad (\text{A.4})$$

making the l.h.s. term of the Eq. (A.3) strictly zero. Now λ stands for the Beltrami parameter related to the composite flow “reduced momentum” for which we seek the solution such that it makes the last term zero on the r.h.s. of the Eq. (A.3) being fully determined by the accretion (i.e. total viscosity effect dominated by photon gas):

$$\mathbf{P}_R (\nabla \cdot \mathbf{P}_I) + \nabla \cdot \mathbf{T} = 0. \quad (\text{A.5})$$

Then, in such minimal model the pressure balance equation (A.3) reduces to a so-called “Generalized Bernoulli Condition”

$$\frac{1}{2} \nabla P_R^2 + \rho_R^2 \nabla (h + \Phi) = 0. \quad (\text{A.6})$$

Hence, the stationary state of the rotating thin composite system of AD can be fully investigated using Eqs. (13,A.4,A.5, A.6) and the explicit form of the viscous stress tensor related to the specific object conditions. Below we employ the model in which the small scale turbulence creates the anomalous dissipation that can be described by using the generalized α -viscosity model introduced by Shakura & Sunyaev (1973) in which we use the effective viscosity model both in the disk and jet as well as in the disk-jet transition areas (Arshilava et al. 2019). In cylindrical coordinates (r, φ, z) describing the disk-jet system, keeping the only significant components $T_{r\varphi}$ and $T_{z\varphi}$ of the viscous stress tensor T_{ik} , assuming the strong azimuthal rotation, splitting the pressure \mathcal{P} into the background constant component \mathcal{P}_0 and deviation form it p ,

$$\mathcal{P} = \mathcal{P}_0 + p, \quad (\text{A.7})$$

the turbulent stress tensor can be split into the background constant component \bar{T}_{ik} and smaller varying deviation t_{ik} :

$$T_{ik} = \bar{T}_{ik} + t_{ik} \quad (\text{A.8})$$

with $\bar{T}_{r\varphi} = \alpha_0 \mathcal{P}_0$. Following Arshilava et al. (2019), assuming axisymmetric flow $v_\varphi = r \Omega_K(r, z)$ rotating locally with Keplerian angular velocity (justified for the rotationally supported flow, for which the radial pressure gradients can be negligible compared to the centrifugal force – situation found for slowly accreting flows with slowly varying background pressure $\mathcal{P}_0 \simeq const$):

$$\Omega_K^2(r, z) = \frac{GM_\star}{(r^2 + z^2)^{3/2}}, \quad (\text{A.9})$$

where M_\star is the mass of the central object, in the axisymmetric case, the viscous stress tensor elements can be calculated as follows:

$$t_{r\varphi} = \frac{r^2}{r^2 + z^2} \beta p, \quad (\text{A.10})$$

$$t_{z\varphi} = \frac{rz}{r^2 + z^2} \beta p, \quad (\text{A.11})$$

where positive/negative p corresponds to the stronger/weaker turbulence compared to the background generalized turbulent steady state.

The geometry of the observed disk-jet structures and the continuity Eq. (15) dictate the expansion of the flow velocity in the following way (Shatashvili & Yoshida 2011; Arshilava et al. 2019):

$$\mathbf{v} = \frac{1}{\rho} (\nabla\psi \times \nabla\varphi) + rv_\varphi \nabla\varphi, \quad (\text{A.12})$$

where the axisymmetric stream function ψ exactly matches the stream function of the actual momentum $\mathbf{P} = \rho\mathbf{v}$ of the bulk flow. Then, the Eq. (A.5) takes the form:

$$\begin{aligned} \frac{v_\varphi}{r} \left(\frac{\partial\psi}{\partial r} \frac{\partial}{\partial z} \ln \rho_R - \frac{\partial\psi}{\partial z} \frac{\partial}{\partial r} \ln \rho_R \right) \\ = \beta \frac{r^2}{r^2 + z^2} \left[\frac{\partial p}{\partial r} + \frac{z}{r} \frac{\partial p}{\partial z} + \frac{2\beta}{r} p \right], \end{aligned} \quad (\text{A.13})$$

and the generalized Bernoulli Condition (A.6) reduces to:

$$\nabla \mathcal{E}_m + \left(v_\varphi^2 + \frac{(\nabla\psi)^2}{r^2 \rho^2} \right) \nabla \ln \rho_R = 0, \quad (\text{A.14})$$

where we have introduced the total mechanical energy

$$\mathcal{E}_m \equiv \Phi + \frac{v_\varphi^2}{2} + \frac{(\nabla\psi)^2}{2r^2 \rho^2}. \quad (\text{A.15})$$

The system of equations describing the relativistic disk-powerful jet equilibrium structure can be closed using the Beltrami condition (A.4) rewritten using the stream function:

$$\begin{aligned} \nabla \times \nabla\psi \times \nabla\varphi + \nabla \times [(\rho r v_\varphi) \nabla\varphi] + \nabla\psi \times \nabla\varphi \times \nabla \ln \rho_I \\ + (\rho r v_\varphi) \nabla\varphi \times \nabla \ln \rho_I = \lambda (\nabla\psi \times \nabla\varphi + (\rho r v_\varphi) \nabla\varphi). \end{aligned} \quad (\text{A.16})$$

Hence, Eqs. (A.13,A.14,A.15) and (A.16) constitute the final set of equations.

To construct the solutions representing disk-jet structure, following Shatashvili & Yoshida (2011), we introduce the orthogonal variables $\tau = z/r$ and $\sigma = \sqrt{r^2 + z^2}$ so that $\nabla\tau \cdot \nabla\sigma = 0$ leading to the obvious results for the Gravitational Potential to be $\Phi = \Phi(\sigma) = -\Omega_0^2/\sigma$ and the stream function to be dependent only on the τ variable ($\psi = \psi(\tau)$): thus, making it possible to separate the variables in the solution. Then, the Eq. (A.13) will take the following form in the similarity variables,

$$v_\varphi \frac{1 + \tau^2}{\sigma^2} \frac{\partial\psi}{\partial\tau} \frac{\partial}{\partial\sigma} \ln \rho_R = \beta \left(\frac{\partial}{\partial\sigma} + \frac{2}{\sigma} \right) \frac{p}{1 + \tau^2}. \quad (\text{A.17})$$

The three components r, φ, z of the Beltrami conditions (A.16), after some straightforward algebra, in the new variables yield

$$\frac{\partial}{\partial\sigma} \left(\frac{\sigma}{(1 + \tau^2)^{1/2}} \rho_R v_\varphi \right) = 0, \quad (\text{A.18})$$

$$\frac{\partial^2 \psi}{\partial\tau^2} + \left(\frac{3\tau}{1 + \tau^2} - \frac{\partial}{\partial\tau} \ln \rho_I \right) \frac{\partial\psi}{\partial\tau}$$

$$= -\lambda \frac{\sigma^3}{(1 + \tau^2)^{5/2}} \rho v_\varphi, \quad (\text{A.19})$$

$$\frac{\partial}{\partial\tau} \ln \left(\frac{\sigma}{(1 + \tau^2)^{1/2}} \rho_R v_\varphi \right) = \lambda \frac{(1 + \tau^2)^{1/2}}{\sigma \rho v_\varphi} \frac{\partial\psi}{\partial\tau}, \quad (\text{A.20})$$

while r and z components of the Generalized Bernoulli Condition (A.6) lead to the following equations, respectively:

$$\frac{1}{\rho} \frac{\partial p}{\partial\sigma} + \frac{\partial \mathcal{E}_m}{\partial\sigma} + 2(\mathcal{E}_m - \Phi) \frac{\partial}{\partial\sigma} \ln \rho_R = 0, \quad (\text{A.21})$$

$$\frac{1}{\rho} \frac{\partial p}{\partial\tau} + \frac{\partial \mathcal{E}_m}{\partial\tau} + 2(\mathcal{E}_m - \Phi) \frac{\partial}{\partial\tau} \ln \rho_R = 0, \quad (\text{A.22})$$

with the total mechanical energy of the composite system $\mathcal{E}_m = \mathcal{E}_m(\sigma, \tau)$. Hence, in similarity variables the physical system of our problem can be analyzed using Eqs. (A.17 - A.22).

We seek the solution of the system assuming that describing physical variables $(p, \rho_I, \rho_R, \lambda)$ can be factorized using the similarity variables (σ, τ) applying variable splitting ansatz (like e.g. $p(\sigma, \tau) = p_1(\sigma)p_2(\tau)$, see (Shatashvili & Yoshida 2011; Arshilava et al. 2019)). For the azimuthal velocity we have:

$$v_\varphi(\sigma, \tau) = V_{\text{Kep}} = \frac{\sigma_0 \Omega_0}{(1 + \tau^2)^{1/2}} \left(\frac{\sigma}{\sigma_0} \right)^{-1/2}, \quad (\text{A.23})$$

where Ω_0 is the Keplerian angular velocity of the rotation at some characteristic radius σ_0 in the disk. Applying this ansatz into Eqs. (A.17-A.22), solving them in σ , we find that the balance of all terms give the explicit solutions for all $(p, \rho_I, \rho_R, \lambda)$ in the σ coordinate. After finding the radial profiles of these parameters above equations represent the ordinary differential equations with respect to τ -variable from which, after straightforward algebra, one obtains (below $\rho_2(\tau) \equiv \rho_{I2}\rho_{R2}$):

$$\beta p_2 = \Omega_0 \sigma_0^{3/2} (1 + \tau^2)^{3/2} \frac{d\psi}{d\tau}, \quad (\text{A.24})$$

$$p_2 \rho_2 + \frac{2}{5} (1 + \tau^2)^3 \left(\frac{d\psi}{d\tau} \right)^2 = \frac{2}{5} \Omega_0^2 \sigma_0^3 \frac{\tau^2}{1 + \tau^2} \rho_2^2, \quad (\text{A.25})$$

from which one derives the defining algebraic equation

$$\beta \left[\beta W(\tau)^2 + \frac{5}{2} \frac{\sigma_0^{3/2} \Omega_0}{(1 + \tau^2)^{3/2}} W(\tau) - \beta \frac{\sigma_0^3 \Omega_0^2 \tau^2}{(1 + \tau^2)^4} \right] = 0 \quad (\text{A.26})$$

for the function

$$W(\tau) \equiv \frac{1}{\rho_2} \frac{d\psi}{d\tau}.$$

As shown in Arshilava et al. (2019), the Eq. (A.26) links the values of β parameter (defining the generalized viscosity of our composite 3-fluid system), τ -dependent part of density ρ_2 and the stream-function ψ , and represents the "realizability" condition for all existing solutions within the considered Beltrami flow model of disk-jet structure formation. There were found three apparent solutions to this equation: 1) one with $\beta = 0$, corresponding to the background dissipation model

($T_{ik} = \alpha_0 \mathcal{P}_0$) and 2) two for $\beta \neq 0$ which for small $\beta \ll 1$ can be approximated by $W_+(\tau)$ (corresponds to disk-solution) and $W_-(\tau)$ (corresponds to the jet one), where

$$W_+(\tau) \approx \frac{2}{5} \beta \sigma_0^{3/2} \Omega_0 \frac{\tau^2}{(1 + \tau^2)^{5/2}} > 0, \quad (\text{A.27})$$

$$W_-(\tau) \approx -\frac{5}{2} \frac{\sigma_0^{3/2} \Omega_0}{\beta} \frac{1}{(1 + \tau^2)^{3/2}} < 0, \quad (\text{A.28})$$

making it possible to find the dependence of the Beltrami parameter λ on the turbulent viscosity parameter β from the Eqs. (A.17 - A.22); moreover, derived two separate solutions grow with β ($\lambda_{\pm} = \lambda(W_{\pm}) \propto \beta$). Illustration for $W(\tau)$ for the three region solution – disk-jet configuration in one solution describing the classes of solutions corresponding to the accretion disk—ejection jet flow (one flow with the matter and total energy) can be found in Arshilava et al. (2019) (see its Figure 2 and related discussion on Beltrami-flow model for disk-jet structure formation). In this model a non-uniformly ($\beta \neq 0$) viscous accreting flow in the disk region ($\tau < \tau_d$) goes through uniformly viscous ($\alpha_0 = \text{const}$, $\beta = 0$) ballistic regime in the transition region ($\tau_d < \tau < \tau_j$) and, finally, into the non-uniformly viscous outflow configuration in the jet region ($\tau > \tau_j$) advecting/dragging the magnetic field.

The general solutions of our weakly magnetized disk-jet model can be calculated as follows (with the general solution $W(\tau)$ of Eq. (A.26) in which β represents the contributions from generalized turbulent viscosity (Shakura & Sunyaev, 1973)):

$$\rho(\sigma, \tau) = \sigma^{-3/2} \rho_2(\tau), \quad (\text{A.29})$$

$$p(\sigma, \tau) = \frac{\sigma_0^{3/2} \Omega_0}{\beta} \frac{(1 + \tau^2)^{3/2}}{\sigma^{5/2}} \rho_2(\tau) W(\tau), \quad (\text{A.30})$$

$$v_r(\sigma, \tau) = -\frac{1 + \tau^2}{\sigma^{1/2}} W(\tau), \quad (\text{A.31})$$

$$v_z(\sigma, \tau) = -\tau \frac{1 + \tau^2}{\sigma^{1/2}} W(\tau). \quad (\text{A.32})$$

Eqs. (A.29-A.32) together with the radial profiles and appropriate choice of the solution for W give the full solution for the disk-jet bulk (ion and electron-photon) flow for different types of density profiles $\rho_2(\tau)$ for which we employ the power-law distribution (cf. Shatashvili & Yoshida 2011):

$$\rho_2(\tau) = A_d (\tau + \tau_0)^{m_d} + A_j (\tau + \tau_0)^{m_j}, \quad (\text{A.33})$$

where parameters A_d , m_d and A_j , m_j define the density profile in the disk and jet regions, respectively. The small parameter $\tau_0 \ll 1$ is used to avoid divergence at the disk center ($\tau = 0$). Hence, Eqs. (A.29-A.32) and (A.33) describe classes of disk-jet solutions within our self-similar Beltrami-flow model.

Substitution of Eqs. (A.27,A.28) into (A.31) and (A.32) yields the velocity field components of the weakly magnetized disk flow.

References

- Arce, H. G., Mardones, D., Corder, S. A., Garay, G., Noriega-Crespo, A., Raga, A. C., 2013 *Aastrophys.J.*, 774, 39
- Arshilava, E. Gogilashvili, M., Loladze, V., Jokhadze, I., Modrekiladze, B., Shatashvili, N.L. Tevzadze, A.G. 2019, *J. High Energy Astrophysics* **23**, 6
- Bai, X-N., 2016 *Astrophys. J.*, 821, 80
- Balbus, S.A. & Hawley, J.F. 1991 *Astrophys. J.*, 376, 214
- Bally, J., 2016 *Ann. Rev. Astron. Astrophys.*, 54, 491
- Balman S. 2020, *ASR* **66**, 5, 1097
- Barnier S., Petrucci, P.-O., Ferreira, J., Marcel, G. 2023 *Astronomische Nachrichten*, 344(4) 20230020
- Baierlein, R., 1978 *MNRAS* **184**, 843
- Barnaveli, A.A., Shatashvili, N.L. 2017 *Astrophys Space Sci.* **362**, 164
- Begelman, M.C., Blandford, R.D., and Rees, M.D. 1984 *Rev. Mod. Phys.* **56** 255
- Begelman, M. C., 1993 "Conference summary", in *Astrophysical Jets*, ed. D. Burgarella et al (Cambridge: Cambridge Univ. Press), 1993, pp. 305-315.
- Begelman, M. C., 1998 *Aastrophys. J.*, 493, 291
- Berezhiani, V.I., Shatashvili, N.L. and Mahajan, S.M. 2019 *Phys. Plasmas* **22**, 022902
- Bisnovatyi-Kogan G. S. and Lovelace, R.V.E., 2007, *ApJ* 667(2), L167-L169
- Blandford, R. D. and Rees, M. J., 1974 *MNRAS*, 169, 395
- Blandford, R. D. and Znajek, R. L., 1977 *MNRAS*, 179, 433
- Blandford, R. D. and Payne, D. G., 1982 *MNRAS*, 199, 883
- Blandford, R. D., 1994 *ApJS*, 90, 515
- Celotti, A. and Blandford, R. D., "Black Holes in Binaries and Galactic Nuclei: Diagnostics, Demography and Formation", in *ESO Astrophysics Symposia* ed. L. Kaper et al. (Berlin, Heidelberg: Springer-Verlag), 2001, 206
- Chan, K. L., & Jones, B. J. T. 1975, *Astrophys. J.*, 200, 454
- Clarke, C. J., and Alexander, R. D., 2016 *MNRAS*, 460, 3044
- Del Santo, M., Pinto, C., Marino, A., D'Al, A., Petrucci, P.-O., Malzac, J., Ferreira, J. Pintore, F. Motta, S. E., Russell, T.D., Segreto, A. and Sanna, A. 2023 *MNRAS* 523, L15–L20
- Dullemond, C. P., Hollenbach, D., Kamp, I., & D'Alessio, P. 2007, in *Protostars and Planets V*, ed. B. Reipurth, D. Jewitt, & K. Keil (Tucson, AZ: Univ. Arizona Press), 555
- Ferreira, J., 1997 *A&A* 319, 340
- Ferreira, J., Dougados, C. and Cabrit, S., 2006 *A&A* 453, 785
- Ferreira, J., Dougados, C. and Whelan, E., 2007 "Jets from Young Stars I: Models and Constraints" in *Lecture Notes in Physics* ed. Ferreira, J. et al. (Berlin, Heidelberg: Springer-Verlag) 2007, 723, 181.
- Ferreira, J. 2008 *New Astronomy Reviews* 52, 42–59
- Harrison, E.R. 1973 *MNRAS* 165, 185
- Hartmann, L., 2009 *Accretion Processes in Star Formation*, Cambridge University Press
- Ioannidis, G., Froebrich, D., 2012, *MNRAS*, 421, 3257
- Kafka, S. & Honeycutt, R.K. 2004 *Astrophys. J.* **128**, 2420
- Kawka, A. and Vennes, S. 2014 *MNRAS* **439**, L90
- Kepler, S. O., Pelisoli, I., Jordan, S., Kleinman, S.J., Koester, D., Külebi, D.B., Pecanha, B.V., Castanheira, B.G., Nitta, A., Costa, J.E.S., Winget, D.E., Kanaan, A. and Fraga, L. 2013 *MNRAS* **429**, 2934
- Koide, S., Shibata, K. and Kudoh, T., 1998 *Astrophys. J.*, 495, L63
- Kotorashvili, K., Revazashvili, N., Shatashvili, N.L. 2020 *Astrophys. Space Sci.*, **365**, 175
- Kotorashvili, K. and Shatashvili, N.L. 2022 *Astrophys. Space Sci.*, **367**, 2
- Krasnopolsky, R., Li, Z. Y. and Blandford, R. D., 1999 *Aastrophys.J.*, 526, 631
- Kudoh, T. and Shibata, K., 1987 *Aastrophys.J.*, 474, 362
- Kuwabara, T., Shibata, K., Kudoh, T. and Matsumoto, R., 2005 *ApJ*, 621, 921
- Lee, C.-F., Li, Z.-Y., Codella, C., Ho, P. T. P., Podio, L., Hirano, N., Shang, H., Turner, N. J., Zhang, Q., 2018 *ApJ*, 856, 14
- Livio, M. "The Formation Of Astrophysical Jets", in *Accretion Phenomena and Related Outflows*; IAU Colloquium 163 ed. D. T. Wickramasinghe et al (San Francisco: ASP) ASP Conference Series 1997, 121, 845.
- Long, K.S., Knigge, C. 2002 *Astrophys. J.* **579**, 725
- Lovelace, R.V.E., Romanova, M.M. and Newman, W.I., 1994, *ApJ*, 437, 136
- Lovelace, R. V. E. 1976, *Nature*, 262, 649
- Mahajan S. M., Nikol'skaya K. I., Shatashvili N. L., Yoshida Z., 2002 *Astrophys. J.*, 576, L161
- Mahajan, S.M., Miklaszewski, R., Nikol'skaya, K.I. and Shatashvili, N.L. 2001 *Phys. Plasmas* **8**, 1340
- Mahajan, S.M., Shatashvili, N.L., Mikeladze, S.V. and Sigua, K.I. 2005 *Astrophys. J.* **634**, 419

Mahajan, S.M., Shatashvili, N.L., Mikeladze, S.V. and Sigua, K.I. 2006 *Phys. Plasmas* **13**, 062902

Matsumoto, R. and Tajima, T. 1995 *Aastrophys.J.*, 445, 767

Matsumoto, r., Machida, M. and Nakamura, K. 2004 *Prog. Theor. Phys. Suppl.* 155, 124

Mignone, A., Plewa, T. & Bodo, G. 2005 *Astrophys. J. Supp.* **160**, 199

Meier, D. L., Edgington, S., Godon, P., Payne, D. G., & Lind, K. R. 1997, *Nature*, 388, 350

Mirabel, I. F., & Rodriguez, L. F. 1994, *Nature*, 371, 46

Mirabel, I.F. & Rodriguez, L.F., 1999 *Annu. Rev. Astron. Astrophys.* 37:409-43

Mouchet, M., Bonnet-Bidaud, J.M., de Martino, D. 2012 *Mem. SAI* **83**, 578

Mukai, K. 2017 *PASP* **129**, 062001

Nordhaus, J., Wellons, S., Spiegel, D.S., Metzger, B.D., Blackman, E.G., 2010 Formation of high-field magnetic white dwarfs from common envelopes, *Proceedings of the National Academy of Sciences*, **108(8)**, 3135

O'Dell, 1981 *Astrophys. J.* 243, L147

Ohsaki, S., Shatashvili, N.L., Yoshida, Z. and Mahajan, S.M. 2001 *Astrophys. J.* **559**, L61;

Ohsaki, S., Shatashvili, N.L., Yoshida, Z. and Mahajan, S.M. 2002 *Astrophys. J. ASTROPHYS. J.*, **570**, 395

Ouyed, R., Pudritz, R. E., & Stone, J. M. 1997, *Nature*, 385, 409

Peebles, P. J. E., 1969, *Astrophys. J.* 155, 393.

Peebles, P. J. E., 1980, *The Large-Scale Structure of the Universe* (Princeton University, Princeton, NJ).

Peebles, P. J. E., 1993, *Principles of Physical Cosmology* (Princeton University, Princeton, NJ).

Pelletier, G., Ferreira, J., Henri, G., & Marcowith, A. 1996, in *Solar and Astrophysical Magnetohydrodynamic Flows*, ed. K. C. Tsinganos (Dordrecht: Kluwer), 643

Phinney, E.S., 1982 *MNRAS* 198, 1109

Pudritz, R. E., & Norman, C. 1986, *Aastrophys.J.*, 301, 571

Puebla, R.E., Diaz, M.P., Hillier, D.J., Hubeny, I. 2011 *Astrophys. J.*, **736**, 17

Shakura, N. I., Sunyaev, R. A., 1973, *A&A*, 24, 337

Shatashvili, N.L. and Yoshida, Z., 2011, *AIPCP*, 1445, 34-53

Shibata, K., & Uchida, Y. 1986, *PASJ*, 38, 631

Smith, M. D., Davis, C. J., Rowles, J. H., Knight, M., 2014, *MNRAS*, 443, 2612

Takahara, F., Rosner, R., & Kusunose, M. 1989, *Aastrophys.J.*, 346, 122

Takasao, S., Suzuki, T.K., and Shibata, K. 2017 *Aastrophys.J.*, 847, 46

Tremblay, P.-E., Fontaine, G., Freytag, B., Steiner, O., Ludwig, H.-G., Steffen, M., Wedemeyer, S. and Brassard, P. 2015 *Astrophys. J.*, **812**, 19

Tout C.A, Wickramasinghe D.T., Liebert J, Ferrario L. and Pringle J.E. 2008 *MNRAS*, **387**, 897

Sikora, M., & Wilson, D.B., 1981 *MNRAS* 197, 529

Spruit, H. C. 2010 *The Jet Paradigm, Lecture Notes in Physics*, 794. Springer-Verlag Berlin Heidelberg, 2010, p. 233

Spruit, H.C. 2011 *AIP Conference Proceedings*, 1381, 227

Uchida, Y., & Shibata, K. 1985, *PASJ*, 37, 515

Ustyogova, G.V., Koldova, A.V., Romanova, M.M., Chechetkin, V.M., Lovelace, R.V.E., 1999 *Astrophys. J.* 516, 221

Yang, H., Yuan, F., Li, H., Mizuno, Y., Guo, F., Lu, R., Ho, L.C., Lin, X., Zdziarski, A.A., Wang, J., 2024 *Sci. Adv.* 10, eadn3544

Yoshida, Z., Shatashvili N. L., 2012, *arXiv:1210.3558*

Vlemmings, W. H. T., Bignall, H. E. and Diamond, P. J. 2007 *ApJ* 656, 198

Zanni, C., Ferrari, A., Rosner, R., Bodo, G. and Massaglia, S., 2007 *A&A*, 469, 811

Zhang, M., Wang, H., Hennings, T., 2014, *AJ*, 148, 26

Weinberg, S., 1972 *Gravitation & Cosmology*, J. Wiley, New York

Widrow, L., 2002 *Rev. Mod. Phys.* **74**, 1

Winget, D.E. and Kepler, S.O. 2008 *Annu. Rev. A&A* **46**, 157